CNWRA *A center of excellence in earth sciences and engineering* ™

A Division of Southwest Research Institute®
6220 Culebra Road • San Antonio, Texas, U.S.A. 78228-5166
(210) 522-5160 • Fax (210) 522-5155

February 25, 2005
Contract No. NRC-02-02-012
Account No. 20.06002.01.352

U.S. Nuclear Regulatory Commission
ATTN: Mrs. Deborah A. DeMarco
Two White Flint North
11545 Rockville Pike
Mailstop T8 A234
Washington, DC 20555

Subject: Programmatic Review of the Paper Titled A Model for Estimating Heat Transfer Through Drift Degradation Based Natural Backfill Materials

Dear Mrs. DeMarco:

The subject paper is being submitted for programmatic review. The paper will be submitted for publication in the proceedings of the 40th U.S. Rock Mechanics Symposium, Alaska Rocks 2005, June 25-29, 2005, Anchorage, Alaska.

The paper presents a model for estimating waste package surface temperature within the potential high-level waste repository at Yucca Mountain. In the approach proposed in this paper, heat transfer through the natural backfill is not by conduction alone, but instead accounts for natural convection as a direct function of the backfill air flow characteristics. The air flow characteristics of the natural backfill material are derived from the rock fall rubble size distribution.

This paper is based on one of the chapters of the Risk Analysis for Risk Insights Progress Report that was recently reviewed and accepted by NRC. The equations and figures presented in this paper are identical to the ones presented in the Risk Analysis for Risk Insights Progress Report.

Washington Office • Twinbrook Metro Plaza #210
12300 Twinbrook Parkway • Rockville, Maryland 20852-1606

Please advised me of the results of your programmatic review. If you have any questions regarding this paper, please contact Dr. Sitakanta Mohanty at 210-522-5185. Your cooperation in this matter is appreciated.

Sincerely,

DRLmm for B. Sagar

Budhi Sagar
Technical Director

cc: W. Reamer
B. Meehan
E. Whitt
B. Leslie
W. Ford
T. McCartin
L. Kokajko
E. Collins
F. Brown
A. Campbell
K. Stablein
M. Bailey
J. Guttmann
A. Csontos
J. Pohle
M. Nataraja
W. Patrick
CNWRA Directors
CNWRA Element Managers
L. Gutierrez

ARMA/USRMS 05-XXX

A MODEL FOR ESTIMATING HEAT TRANSFER THROUGH DRIFT DEGRADATION BASED NATURAL BACKFILL MATERIALS

Sitakanta Mohanty
Center for Nuclear Waste Regulatory Analyses
Southwest Research Institute®
San Antonio, Texas, USA

George Adams
Center for Nuclear Waste Regulatory Analyses
Southwest Research Institute
San Antonio, Texas, USA

ABSTRACT: This paper presents a model for estimating waste package surface temperature within the potential high-level waste (HLW) repository at Yucca Mountain, Nevada, USA. In the current repository design, HLW will be disposed in waste packages that will be emplaced in unbackfilled horizontal drifts excavated nearly 350 m [1,148 ft] below the ground surface. As part of this model, the natural degradation of the drift is considered. In this case, natural drift material dislodged from the drift ceiling (natural backfill) is likely to accumulate on the drift floor and surround the drip shield, insulating the engineered components (i.e., limiting convective and radiative heat transfer), and thereby elevating the temperature at the waste package surface. In the approach proposed in this paper, heat transfer through the natural backfill by conduction and convection is considered. The air flow characteristics of the natural backfill material are derived from the particle size distribution. Conduction and convection through the natural backfill results in a lower overall waste package surface temperature than that of conduction alone, but the lowering of the temperatures appears to be strongly controlled by the mean particle diameter and porosity.

1. INTRODUCTION

One of the key aspects of assessing the performance of the repository is the estimation of the temperature of the engineered system and the surrounding medium in the current design of the potential repository at Yucca Mountain, Nevada, is. According to the current design, the repository horizon will be located 350 m [1,148 ft] below the ground surface, and the heat-generating spent-nuclear fuel will be disposed in waste packages emplaced in drifts excavated in the rock. The drifts will not be backfilled after the emplacement of waste packages. In addition, the engineered supports for the drift are designed to perform their intended function for preclosure period only [1].

Current NRC and Center for Nuclear Waste Regulatory Analyses (CNWRA) calculations of the degradation of mined openings suggest that as much as 100 percent of the drifts may degrade during the first 1,000 years after repository closure [1, 2]. The natural drift material dislodged from the drift roof, henceforth referred to as natural backfill, is likely to accumulate on the drift floor and gradually surround the drip shield. The insulating effect of the natural backfill material is likely to increase drip shield, waste package, and wasteform temperatures. High temperatures may adversely affect the load-bearing capacity of the drip shield and the waste package, thus increasing their failure potential during the period of high temperatures. The increased temperature at later times may also accelerate drip shield and waste package corrosion and wasteform dissolution, if moisture is present.

The DOE calculations with engineered backfill at repository closure, which can be viewed as a surrogate for natural backfill, suggest the estimated peak waste package temperature may increase from nearly 165 to 315 °C [329 to 599 °F] [3], and temperatures of other components of the engineered system may increase correspondingly. The NRC independent analyses also estimate a similar increase in temperature at the waste package surface. For example, making a conduction-only assumption for heat transfer through the backfill material [4,5] estimated a peak temperature of approximately 351 °C [664 °F]. These three calculations suggest the estimated peak temperature at the waste package could be nearly 185 °C [333 °F] higher in the presence of backfill material than the no-backfill case.

The temperatures estimated in [3,4, 5] are based on the key assumption that the engineered backfill is representative of natural backfill.

Constraining the heat transfer assumption for the backfill material to conduction-only implies the backfill layer may behave as a thermal blanket at all temperatures. It may be argued that analyses with high temperatures likely bound the adverse effects of temperature on water chemistry, rock stability, and drip shield/waste package corrosion rates. However, that is debatable because of the beneficial effect of high temperatures that keep water from contacting the waste package for a prolonged period. Consequently, this analysis develops an alternative thermal model to estimate the effect of drift degradation on near-field temperature evolution.

This paper presents the mathematical model for evaluation of waste package surface temperature throughout the immediate space surrounding the potential repository for 10,000 years during active natural backfilling of the drift due to drift degradation. Section 2 of this paper provides a brief description of the repository site and the repository environment. Section 3 presents the methodology for estimating temperature at the waste package. Section 4 presents assumptions. Section 5 describes results from the deterministic and stochastic calculations. Section 6 presents the conclusions.

2. DESCRIPTIONS OF PROPOSED SITE AND REPOSITORY

Yucca Mountain is 40 km [24.85 mi] long by 6–10 km [3.73–6.21 mi] wide. The stratigraphy at Yucca Mountain is composed of a gently dipping sequence of ash-flow tuffs, lavas, and volcanic breccias more than 1,800 m [5,905 ft] thick. A subparallel series of ridges controlled by steeply dipping faults dominates the mountain. The rock unit being considered for the potential repository facility is a densely welded ash-flow tuff of the Topopah Spring member of the Paintbrush Tuff. The mountain crest varies between altitudes of 1,500 m [4,921 ft] and 1,930 m [6,323 ft] and is nearly 650 m [2,133 ft] higher than the floor of Crater Flat to the west of the site. The depth of the groundwater table from the repository horizon is approximately 350 m [1,148 ft] directly below the repository block. Climate at the site is generally arid to semiarid, with an average precipitation of nearly 180 mm/yr [7 in/yr].

The potential repository at Yucca Mountain is an underground facility designed to accommodate 70,000 metric tons of HLW. The waste disposed in the repository is expected to consist of both commercial SNF (~90 percent in terms of activity) and defense and other HLW (~10 percent in terms of activity), with an age of 5-50 years. The specific layout of the underground facility used for this study is based on the DOE new Enhanced Design Alternative (EDA) II, also referred to as the Hot Drift Cool Pillar design [6]. The relevant EDA-II design specifications are presented in Table 1. DOE intends to place the drifts far enough apart so that a significant portion of the pillars may remain below the boiling temperature for water to facilitate infiltrating and thermally driven water above the repository to flow through the cool pillars. The

Table 1. Relevant repository design information [6]

Selected design characteristics	EDA-II
Design basis areal mass loading	60 MTHM/acre
Emplacement area	~1,050 acres
Drift spacing	81 m (center to center)
Drift diameter	5.5 m
Invert	Crushed tuff ballast in and around a steel frame
Number of waste packages (based on various waste types)	10,039
Total length of emplacement drifts	54 km
End-to-end distance between waste packages in a drift	0.1 m
Waste package materials	2 cm Alloy 22 over 5 cm Type 316L SS
Maximum waste package capacity	21 pressurized water reactor assemblies
Drip shield	2 cm thick Ti-Grade 7
Designed emplacement backfill	None, but natural backfilling could occur
Preclosure period	50 yr
Preclosure ventilation rate (50 yr)	15 m^3/s air flow in emplacement drifts

rock in the immediate vicinity of the drifts may be heated above boiling, which may reduce seepage into the drift during the thermal period; thus, drift spacing, waste package spacing, blending of the waste types, and active ventilation before closure are the design criteria to control temperature and limit seepage into the drifts.

Waste package, drip shield, and invert are the key engineered barriers in EDA-II. The waste package design for HLW disposal consists of a large cylinder (i.e., approximately 1.8-m diameter and 5.3-m length) that includes a 20-mm-thick Alloy 22 outer overpack and a 50-mm-thick Type 316L stainless steel (SS) inner overpack in the drift on v-shaped supports. All are emplaced on an invert (i.e., a platform). A drip shield, made of Titanium Grade 7, covers the top and sides of the waste package and extends the length of the emplacement drift. The drip shield is intended to prevent dripping on the waste package surface, especially during the thermal reflux period when environmental conditions could be conducive to localized corrosion. Prior to repository closure, active ventilation of the drifts will reduce the relative humidity and remove a substantial fraction of the heat emitted by the waste and, thus, keep temperature below the threshold at which cladding failure could occur.

3. METHODOLOGY

The methodology developed for this analysis directly links heat transfer to natural convection, which is derived from natural backfill characteristics. Because the temperatures are estimated as a function of heat transfer regimes (i.e., the conduction- versus convection-dominated regimes) explicitly, the approach eliminates the assumption that heat transfer in the natural backfill is from stagnant conduction only (i.e., no natural convection). The heat transfer regimes are determined from the air flow characteristics of the natural backfill medium, which are derived from the particle size distribution.

This section describes estimations of the (i) heat transfer regime; (ii) natural backfill permeability, which is used in determining flow characteristics; (iii) significance of the convection regime; and (iv) temperature based on appropriate flow regimes.

3.1. Estimation of Convective Heat Transfer

3.1.1 Rayleigh Number

When there is no backfill between the drip shield and the drift wall, radiation and convection heat transfer are likely to occur in the air gap. When the backfill material is present, generally radiation heat transfer will be neglected within the backfill because there are small temperature differences across air gaps within the backfill material itself. Depending on the nature of natural backfilling, however, convective heat transfer may occur because of buoyant forces from heated air contained in the pore spaces near the waste package. The Rayleigh number, which expresses the ratio of the transport of energy by free convection to the transport by conduction, may be used to establish the condition for the onset of free convection. Convection currents may develop when the temperature gradient exceeds a critical value, but the temperature that establishes natural convection in air may not be sufficient to establish natural convection in air in a porous medium, largely because the viscous drag of the solids on the fluid may lead to small apparent velocities [7].

The approach used in this analysis is a physics-based model. For this model, convective heat transfer in the region with backfill is based on porous media petrophysical characteristics that relate radial heat transfer to natural convection in an annular region. The onset of natural convection and the heat transfer rates are related to the permeability of the natural backfill material. The permeability is estimated from porosity and particle size distribution of the natural backfill material.

Convection in the annular region between two horizontally emplaced concentric cylinders, with the inner cylinder temperature being higher, may be characterized by [7]

$$\mathrm{Ra} = \frac{g\beta\left(T_{do} - T_{bfo}\right)r_i^3}{\nu\alpha_m} \qquad (1)$$

where

Ra — Rayleigh number [unitless]
g — Acceleration caused by gravity [m/s^2]
β — Volume of thermal expansion [1/K]

r_i — Backfill inner radius [m]
ν — Kinematic viscosity [m^2/s]
α_m — Thermal diffusivity [m^2/s]
T_{bfo} — Lower temperature at the backfill outer surface [K]
T_{do} — Higher temperature at the backfill inner surface [K]

If the space between the outer and inner cylinders is filled with a porous medium, the Rayleigh number may be expressed by

$$Ra_{r_i} = g\beta Kr_i \frac{T_{do} - T_{bfo}}{\nu\alpha_m} \qquad (2)$$

where K is the permeability (m^2) of the porous medium [8] and Ra_{ri} is the Rayleigh number for concentric cylinders filled with a porous medium. The onset of free convection in porous media may occur at or above Rayleigh numbers of the order of $4\pi^2$ (i.e., $Ra_c > 39.5$, where Ra_c is the Rayleigh number corresponding to the onset of free convection) [8]. This criterion is based on horizontal layers filled with nonmoving fluid and upper and lower boundaries that may be both impermeable to flow and isothermal.

In Eq. (2), K and α_m are functions of the characteristics and the accumulation pattern of the natural backfill material. The parameter K for the natural backfill may be determined from bulk physical properties (i.e., textural quantities such as grain size, sorting, packing, and particle size distribution).

3.1.2 Estimation of Permeability (K)

A physics-based model is used in this analysis to estimate the permeability of the accumulated natural backfill. This model estimates permeability using the model proposed by Panda and Lake [9], particle size distribution statistics and other properties (e.g., porosity, tortuosity, and such) in the Carman-Kozeny equation.

Permeability of a medium, which is an assembly of a distribution of spherical particle sizes, may be represented by [9]

$$K = \frac{\overline{D}_p^2 \phi^3}{72\tau(1-\phi)^2}\left[\frac{\left(\gamma C_{D_p}^3 + 3C_{D_p}^2 + 1\right)^2}{\left(1 + C_{D_p}^2\right)^2}\right] \qquad (3)$$

where

C_{D_p} — Coefficient of variation of the particle size distribution = $\sigma_{D_p} / \overline{D}_p$ [unitless]
σ_{D_p} — Standard deviation of a particle size distribution [m]
ϕ — Porosity (bulk property) [unitless]
$\overline{D}_p$ — Mean particle diameter [m]
τ — Tortuosity of the medium (bulk property) [unitless]
γ — Skewness of a particle size distribution [unitless]

This equation is valid for any particle size distribution type. When $C_{D_p} = 0$, the terms in the square bracket vanish, and Eq. (3) reduces to the Carman-Kozeny equation, an equation that estimates the permeability of an assembly of single-size spheres of diameter D_p.

Parameters $\overline{D}_p$ and C_{D_p} in Eq. (3) may be derived from measurements. But as mentioned in [9], measured data typically are reported as median grain size, $D_{p_{med}}$ (instead of $\overline{D}_p$), and Trask sorting coefficient, S_0 (instead of C_{D_p}). The experiments are typically based on a weight statistic that is usually determined from a sieve analysis, in comparison to the equations based on number statistics [10, 11]. Sieve analysis results use the Φ - distribution. In this approach, the particle size distribution is described through Φ classes, and each Φ class is described by the weight fraction. Here, $\Phi = -\log_2 D_p$ represents the Φ - distribution and its attributes

$$\overline{D}_p = \exp\left\{-\left[\overline{\Phi}(ln\,2) + 2.5\sigma_\Phi^2 (ln\,2)^2\right]\right\} \qquad (4)$$

where $\overline{\Phi} = -\log_2 D_{p_{med}}$ for a Φ normal distribution

and $D_{P_{med}}$ is in millimeters.

$$\sigma^2_{D_p} = \exp\left\{-\left[2\overline{\Phi}(ln2) + 4\sigma^2_{\Phi}(ln2)^2\right]\right\} \quad (5)$$

where

$$\sigma_{\Phi} = \frac{\overline{\Phi} S_0^2 - \overline{\Phi}}{0.675 + 0.675 S_0^2} \quad (6)$$

and S_0 is the Trask sorting coefficient [11], which is defined as

$$S_0 = \sqrt{F_{\Phi_m} / F_{\Phi_m}} \quad (7)$$

where F represents the weight fraction.

Equations (4) through (6) assume that the particle size distribution is statistically isotropic and homogeneous. As these equations show, C_{D_p} is a function of S_0 and the median grain size. C_{D_p} increases with S_0 for a given $\overline{D}_p$. This increase is slow if the particle sizes are poorly sorted. In the limit of extremely poor sorting, C_{D_p} appears to be independent of sorting.

3.1.3. Determining the Significance of the Convection Regime

For a horizontal layer of porous medium of thickness L and width h heated from below when Ra exceeds the critical value $Ra_c \approx 39.5$, the Nusselt number is given by

$$Nu_L = \frac{hL}{K} = \frac{Ra_L}{40} \text{ when } Ra_L \geq 40, \text{ else } = 1 \quad (8)$$

The Nusselt number is defined as the ratio of the heat transport with and without convection. From Eq. (8) shows the relationship between Nu, K, and Ra. The Nusselt number of a horizontally emplaced annulus of porous medium with a heat source located at the inner surface of the annulus may be represented by the following correlation:

$$Nu \cong 0.44 Ra_{r_i}^{1/2} \frac{ln(r_o / r_i)}{1 + 0.916(r_i / r_o)^{1/2}} \quad (9)$$

where

r_o — Outer radius of annulus
r_i — Inner radius of annulus

The correlation in Eq. (9) [12] was obtained from experiments by Caltagirone [13] and is appropriate for $1.19 \leq \frac{r_o}{r_i} \leq 4$. The correlation is valid for Nu >>1. The outer surface of the natural backfill material may be viewed as the outer wall of the annulus, and the drip shield outer wall may be considered as the inner wall of the annulus.

3.2. Temperature Calculation

Figure 1 shows the schematic and an idealization of the cross section of a drift with a waste package, drip shield, backfill, and invert used to calculate temperatures in the drift. Temperature calculations use the same basic formalism presented in [5] except for a few modifications, as shown in Eq. (10). The steady-state temperature drop in the drift (invert is deliberately omitted in the equations for simplicity) is estimated from the rock wall temperature, and may be represented by

$$T_{wp} - T_{rw} = \frac{q}{2\pi wpl}\left[\frac{ln\left(\frac{r_{rw}}{r_{bfo}}\right)}{k_{cv2} + k_{r2}} + \frac{ln\left(\frac{r_{bfo}}{r_{dso}}\right)}{k_{bf}} + \frac{ln\left(\frac{r_{dso}}{r_{dsi}}\right)}{k_{ds}} + \frac{ln\left(\frac{r_{dsi}}{r_{wp}}\right)}{k_{cv1} + k_{r1}}\right] \quad (10)$$

where

k — Equivalent thermal conductivity [W/m-K]
T — Surface temperature [K]
q — Heat flux above the waste package [W]
wpl — Waste package spacing [m]

The rock wall temperature, T_{rw}, is estimated using a mountain-scale analytical heat conduction model which is separate from the in-drift model discussed

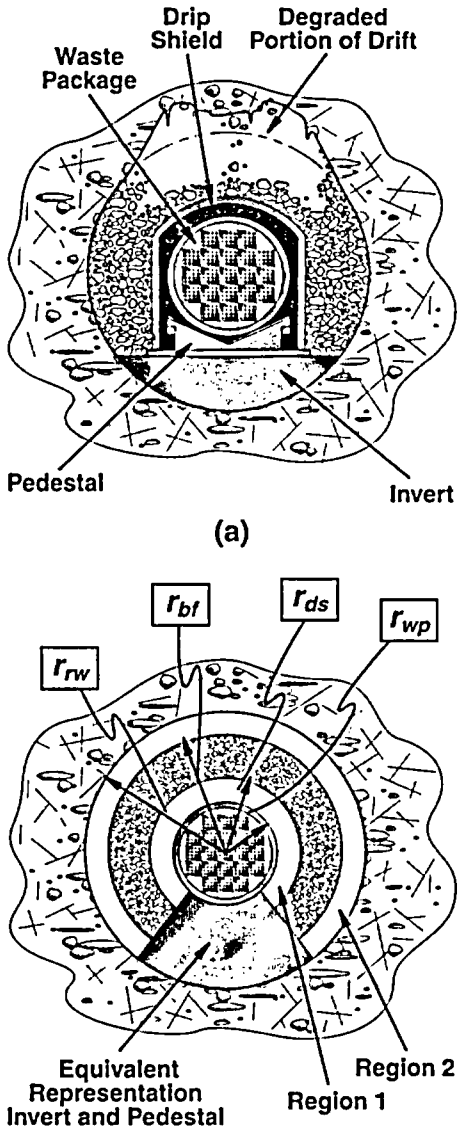

Figure 1. Schematic Showing (a) Natural Backfilling from Drift Degradation and (b) Idealization of Natural Backfilling for Computing Heat Transfer

in this paper. Numerical notations 1 and 2 in the subscripts represent Region 1 (the region between the waste package and the drip shield) and Region 2 (the region between the drip shield and the rock wall).

Character notations waste package, rw, bf, bfo, ds, dsi, dso, cv, and r refer respectively to waste package, rock wall, backfill, backfill outer surface, drip shield, drip shield inner surface, drip shield outer surface, convection, and radiation. Equations used to estimate the equivalent conductivities, k_{cv1}, k_{r1}, k_{cv2}, k_{r_s}, and k_{bf}, are presented next (k_{ds} is a constant).

The convective heat transfer from natural convection in the unbackfilled region is represented explicitly and is based on temperature, Prandtl number [Pr], acceleration because of gravity, and volume of thermal expansion [14, 15]. This model replaces the previously [5] assumed equivalent thermal conductivity for convective heat transfer, a fixed value that is 30 times the air thermal conductivity

$$k_{cv1} = 0.386 k_{air} \left(\frac{\mathrm{Pr}}{0.861+\mathrm{Pr}}\right)^{1/4} \left[\frac{\left(\ln\frac{D_{dsi}}{D_{wp}}\right)^4 g\beta\left(T_{wp}-T_{dsi}\right)}{\nu\alpha\left(D_{wp}^{-3/5}+D_{dsi}^{-3/5}\right)^5}\right]^{1/4} \quad (11)$$

$$k_{cv2} = 0.386 k_{air} \left(\frac{\mathrm{Pr}}{0.861+\mathrm{Pr}}\right)^{1/4} \left[\frac{\left(\ln\frac{D_{rw}}{D_{bfo}}\right)^4 g\beta\left(T_{bfo}-T_{rw}\right)}{\nu\alpha\left(D_{bfo}^{-3/5}+D_{rw}^{-3/5}\right)^5}\right]^{1/4} \quad (12)$$

The radiative heat transfer between concentric cylinders may be represented by

$$k_{r1} = \frac{\ln\left(\frac{r_{dsi}}{r_{wp}}\right)\sigma r_{wp}\left(T_{wp}^2+T_{dsi}^2\right)\left(T_{wp}+T_{dsi}\right)}{\frac{1}{\epsilon_{wp}}+\frac{1-\epsilon_{dsi}}{\epsilon_{dsi}}\left(\frac{r_{wp}}{r_{dsi}}\right)} \quad (13)$$

and

$$k_{r2} = \frac{\ln\left(\frac{r_{rw}}{r_{bfo}}\right) r_{bfo}\left(T_{bfo}^2+T_{rw}^2\right)\left(T_{bfo}+T_{rw}\right)}{\frac{1}{\epsilon_{bfo}}+\frac{1-\epsilon_{rw}}{\epsilon_{rw}}\left(\frac{r_{bfo}}{r_{rw}}\right)} \quad (14)$$

where

σ — Stefan-Boltzman constant (5.67×10^{-8} w/cm^2 - K^4)
ϵ — Emissivity [unitless]

Heat transfer in the backfill is represented by

$$k_{bf} = k_{eff} = \frac{q'}{2\pi} \frac{ln\left(\frac{r_o}{r_i}\right)}{T_{do} - T_{bfo}} \quad (15)$$

where

$$q' = \mathrm{Nu} \cdot q_c \quad (16)$$

and

$$q_c = 2\pi k_m \frac{T_{do} - T_{bfo}}{ln\left(\frac{r_o}{r_i}\right)} \quad (17)$$

Parameters such as k_{r1}, k_{r2}, k_{bf}, k_{cv1}, and k_{cv2} on the right-hand side of Eq. (10) are functions of temperature for which this equation is solved. Although this equation may be simplified for obtaining a solution explicitly, obtaining such a solution is rather cumbersome (involving a fourth-order equation). An iterative solution was therefore, used to solve Eq. (10) to obtain waste package temperature. The iterative solution of the Brent method [17] permits explicit incorporation of the temperature dependency of convection. Heat transfer ca, therefore, be computed as a function of the heat transfer regime.

To represent time-dependent drift degradation, the backfill thickness was varied as a function of time, as implemented in Manepally[1]. The backfill thickness is not allowed to exceed the gap between the undegraded drift and the drip shield (see the horizontal line in Figure 2).

4. ASSUMPTIONS

The following assumptions were incorporated into the model pertaining to (i) heat transfer calculations, (ii) geometric simplifications before and during drift degradation, and (iii) natural backfill characteristics. Additional assumptions may be found in Chapter 5 in [18].

[1]Manepally, C., R. Fedors, G. Adams, R. Green, and D. Gute. 2003. Effects of drift degradation on environmental conditions in drifts. *Presentation at the 2003 American Geophysical Union Fall Meeting, San Francisco, 8–12 December 2003.*

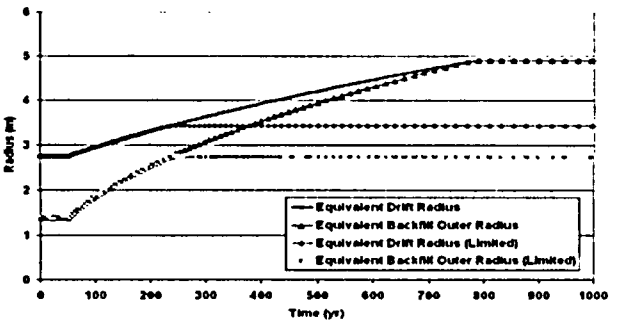

Figure 2. Equivalent Drift Radius and Backfill Radius as a Result of Drift Degradation and Natural Backfilling of the Drift[2]

4.1. Heat Transfer Assumptions

- Heat transfer through various engineered components in the drift (e.g., waste package, invert, backfill, and drip shield) is quasi-steady state.
- Heat transfer along the drift is negligible. This assumption is an artifact of the use of an entire line of waste packages in a drift as a line source. This assumption implies limited variation at the waste package scale.

4.2. Geometric Simplifications

- The engineered components inside the drift are idealized assuming the waste package is coaxial with the drift, the invert is a wedge occupying 25 percent of the drift volume, and the drip shield is circular and coaxial with the drift.
- The natural backfill material around the drip shield may be idealized as a concentric annular region coaxial with the waste package and drip shield limited in thickness (see the horizontal lines in Figure 2) to the original distance between the drift wall and the outer surface of the drip shield. This assumption implies that drift degradation is relatively homogeneous. It is likely that certain portions of the drift may have no rubble accumulation, whereas, other sections may be filled with rubble.

[2]Ibid.

- The fallen material is sufficient to fill the drift and the void created as a result of drift degradation. Figure 1 illustrates drift degradation for a partially degraded drift with the fallen material surrounding the drip shield.

4.3. *Backfill Material Assumptions*

- The natural backfill material may remain unconsolidated during the entire simulation period. Consolidation (e.g., cementation) may decrease convective heat transfer and may increase conductive heat transfer. The net result is a likely increase in waste package temperature compared to the unconsolidated backfill case.

- The permeability of the natural backfill material is greater than 1 darcy ($\sim 1 \times 10^{-12}$ m^2). The permeability model in Eq. (3) is generally not applicable for permeability less than 1 darcy [9].

- Particles are spherical, and particles with a range of diameters are present in the system. Though the model is based on spherical particles, the effect of nonspherical particles may be captured by varying porosity, because the nonsphericity and spheroid eccentricity may have the greatest impact on porosity [18].

- The natural backfill material satisfies statistical homogeneity.

5. RESULTS

The model presented in Section 3 was implemented in the Total-system Performance Assessment (TPA) code [17], and the temperature at the waste package was computed. The temperature behavior was investigated for various arbitrarily chosen natural backfilling conditions (e.g., time of backfill, volume of backfill, and such). Nominal values used in these calculations are presented in Table 2. Because an important aspect of this study was to determine if natural (free) convection in the natural backfill influences the estimated waste package temperature, the flow characteristics of the natural backfill material were investigated as a function of mean particle size, $\overline{D}_p$; porosity, ϕ; tortuosity, τ; coefficient of variation, C_{D_p}; and skewness of the distribution, γ, characterizing the particle size distribution.

Table 2. Parameter Names and Values

Symbol	Parameter	Value
wpl	Waste package spacing	6.14 m
k_{ds}	Drip shield thermal conductivity	20.77 W/(m-°C)
bth	Backfill thickness	0–1.36 m
D_{rw}	Drift diameter	5.5 m
D_{wp}	Waste package diameter	1.579 m
D_{si}	Drip shield internal diameter	2.75 m
D_{so}	Drip shield outer diameter	2.78 m
D_{bfi}	Backfill internal diameter	D_{so} m
D_{bfo}	Backfill outer diameter	$D_{so} + 2 \times bth$ m
σ	Stefan-Boltzman constant	5.67×10^{-8} W/(m^2-K^4)
ε_{wp}	Emissivity of waste package surface	0.87
ε_{bfo}	Emissivity of backfill outer surface	0.8
ε_{rw}	Emissivity of drift wall	0.8
ε_{dsi}	Emissivity of drip shield internal surface	0.63
L	Waste package length	5.275 m
β	Volume of thermal expansion	0.00285 1/K
ν	Kinematic viscosity	32.39×10^{-6} m^2/s
g	Acceleration caused by gravity	9.81 m/s^2

Table 2. Parameter Names and Values (continued)

γ	Skewness of a particle size distribution	0–1.5
τ	Tortuosity of the medium	1.25–3.0
C_{D_p}	Coefficient of variation of the particle size distribution	0.1–0.6
k_{air}	Thermal conductivity of air	0.0373 W/(m-°C)
S_o	Trask sorting coefficient	2.0
α_m	Thermal diffusivity	3.417×10^{-4} m²/s
k_m	Thermal conductivity of the backfill	0.27 W/(m-K)
Pr	Prandtl number	0.7
ϕ	Porosity	0.1 – 0.6
$\overline{D}_p$	Mean diameter of backfill particle	0.1 – 0.5 m

5.1. Air Flow Characteristics of the Natural Backfill Material

Estimates of permeability were first performed without any distributional assumptions for the natural backfill material particle sizes. The permeability was then estimated assuming a Φ -normal distribution for the particle sizes. Following are the key observations using Eq. (3):

- Permeability, K, increased with an increase in $\overline{D}_p$. $\overline{D}_p$ was varied between 100 and 500 mm [0.33 and 1.64 ft] at various ϕ values (0.1 and 0.6), while keeping other parameters fixed $\{\tau = 2.5, \gamma = 0.25, \text{and } \sigma_{D_p} = 60\,\text{mm}[0.2\,\text{ft}]\}$. σ_{D_p} was adjusted in such a manner that C_{D_p} could be maintained at 0.6. Parameters and ϕ contributed most to the increase in the estimated permeability.
- Permeability increased with an increase in C_{D_p}. C_{D_p} was varied between 0.1 and 0.6 at various ϕ values. Other parameters were fixed $\{\tau = 2.5, \gamma = 0.25, \text{and } \overline{D}_p = 100\,\text{mm}\,[0.33\,\text{ft}]\}$. σ_{D_p} was varied in such a manner that the desired C_{D_p} values were obtained. Permeability increased with C_{D_p}, but not as dramatically as with $\overline{D}_p$ and porosity.
- Permeability increased with an increase in γ. γ was varied between 0 and 1.5 at various ϕ (0.1 and 0.6). Other parameters were fixed $\{\tau = 2.5, \overline{D}_p = 100\,\text{mm}\,[0.33\,\text{ft}], \text{and } \sigma_{D_p} = 60\,\text{mm}\,[0.2\,\text{ft}]\}$. Permeability increased with γ, but not as dramatically as with $\overline{D}_p$, ϕ, and C_{D_p}.
- Results from the Φ -normal distribution example: $D_{p_{med}}$ was specified at 1,000 mm [3.28 ft], and the sorting coefficient, S_0, was varied between 1 and 1.25. $\overline{D}_p$ and σ_{D_p} were obtained from $D_{p_{med}}$ and S_0 as shown in Eqs. (4) through (6). When the particles were well sorted (i.e., $S_0 = 1$), a permeability value of 255.1 mm² (2.58×10^8 darcy) was obtained, but as S_0 was increased, the permeability value rapidly decreased. At $S_0 = 1.25$, the estimated permeability was 6.93×10^{-7} mm² (0.702 darcy). Similar calculations were performed at higher S_0 and D_p values. The effect of ϕ, S_0, and $\overline{D}_p$ were studied using $\phi = 0.5$, $S_0 = 2$, and $D_{p_{max}} = 5{,}000\,\text{mm}[16.4\,\text{ft}]$. τ has only a moderate influence on the estimated K.

$\overline{D}_p$ and ϕ have a much greater impact on K than C_{d_p}, γ, τ. A high K leads to a high Ra [Eq. (2)]. Previous analyses suggest the permeability may be high enough in many cases to give rise to high Ra and Nusselt numbers, implying likely substantial heat transfer by natural convection.

5.2. *Temperature Calculations*

Because the characteristics of the natural backfill material are uncertain, several likely bounding and representative calculations were performed to understand the trend in temperature evolution as a function of time.

Figures 3 and 4 show the effects of mean particle diameter, $\overline{D}_p$, and porosity, ϕ, on estimated waste package temperature. The sharp rise in temperature at 50 years pertains to the beginning of the postclosure period, which is associated with the end of the ventilation period. The mean particle diameter was varied between 0.1 and 0.5 m [0.33 and 1.64 ft] (Figure 3). The porosity was varied between 0.1 and 0.6 (Figure 4). Other parameters were set to their mean values. Of the two parameters, porosity had a greater effect on estimated waste package temperature than did the mean particle diameter. Analyses also were performed in which skewness, tortuosity, and the coefficient of variation of the particle size distribution were varied. These three parameters had a much smaller effect on estimated waste package temperature.

Figures 5 and 6 show the estimated temperature evolution using 450-realization Monte Carlo runs in which various parameters were sampled from

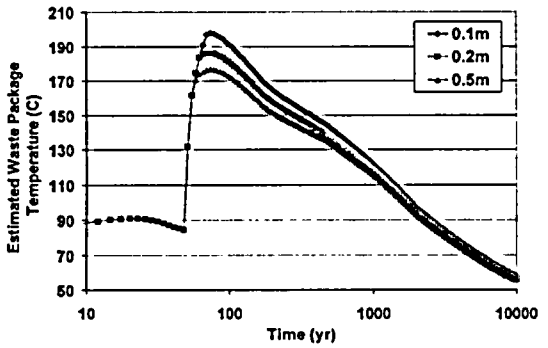

Figure 3. Estimated Variation in Waste Package Surface Temperature at Different Mean Particle Diameters of the Natural Backfill from Mean Value TPA Code Simulations

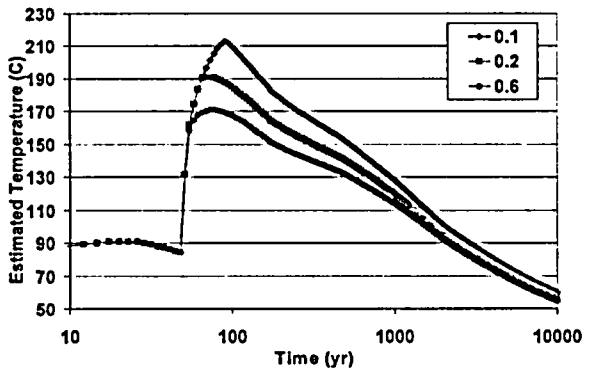

Figure 4. Estimated Variation in Waste Package Surface Temperature at Different Porosities of the Natural Backfill from Mean Value TPA Code Simulations

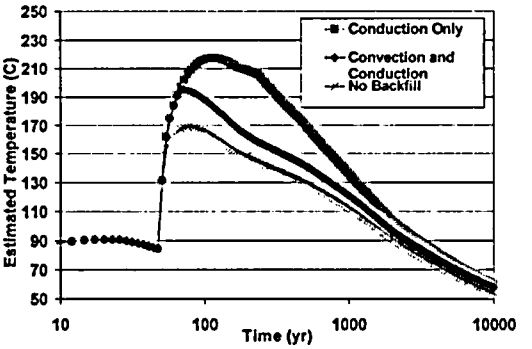

Figure 5. Estimated Evolution of Waste Package Temperature for Subarea 1 as a Function of Various Assumptions Regarding Heat Transfer in the Natural Backfill with Each Curve Representing the Average Temperature from 450 Monte Carlo Realizations

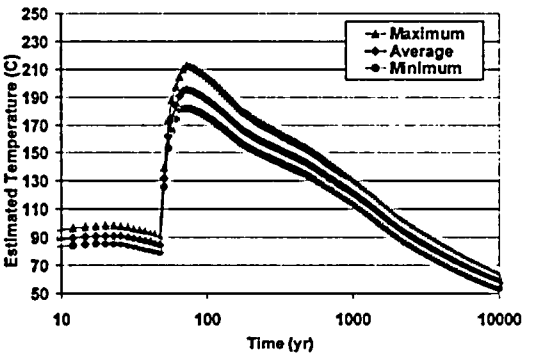

Figure 6. Estimated Average, Minimum, and Maximum Waste Package Surface Temperatures for Subarea 1 from 450 Monte Carlo Realizations

assigned ranges: particle diameter {0.1–0.5 m [0.33–1.64 ft]}, porosity (0.1–0.6), tortuosity (1.25–3.0), skewness (0.0–1.5), and coefficient of variation 0.1–0.6. For these parameters, uniform distributions were used. Figure 5 shows the average waste package temperature from 450 realizations for three cases: conduction only, convection and conduction, and no backfill.

Similar to the previous two figures, the abrupt rise in estimated temperature at 50 years corresponds to the end of the ventilation period. As shown in this figure, the estimated peak mean temperature for the combined convection and conduction heat transfer mode is 195 °C [383 °F] and occurs at 73 years (i.e., 23 years after repository closure). The estimated peak mean temperature for conduction is only 217 °C [423 °F] and occurs at 118 years (i.e., 68 years after repository closure). These estimated peak mean temperatures are within 22 °C [40 °F] of each other, with the combined mode having the lower estimated peak mean temperature.

Figure 5 also shows that, as convection occurs, the estimated peak mean waste package temperature shifts to earlier times. The estimated peak mean temperature for the combined mode occurs 45 years earlier than when conduction alone is assumed. Figure 6 shows the range of estimated waste package temperatures for variation in input parameters using 450 Monte Carlo realizations. The lowest estimated peak temperature is 182 °C [360 °F], while the highest is 213 °C [415 °F]. This difference represents a 31-°C [56-°F] increase in the estimated peak temperature over the parameter ranges specified.

These analyses suggest the estimated waste package temperature can be sensitive to the heat transfer characteristics of natural backfill material. As Figures 3 and 4 suggest, the two key parameters anticipated to govern heat transfer in the backfill are mean particle diameter and porosity.

Heat transfer calculations suggest the estimated waste package temperature may be in between the value obtained from the no-backfill condition and the case with the conduction-only heat transfer in the natural backfill.

6. CONCLUSIONS

The drifts in the potential repository at Yucca Mountain may degrade throughout the potential repository. One way that drift degradation may affect repository performance is by increasing the repository temperature including the drip shield, waste package, and wasteform temperatures. The increased temperature at later times also may accelerate drip shield and waste package corrosion and wasteform dissolution. High temperatures may adversely affect the load-bearing capacity of the drip shield and the waste package, thus increasing the failure potential during the period of high temperatures.

Bounding analyses using an engineered backfill as a surrogate for natural backfill estimated a substantial increase {from 165 to 351 °C [329 to 664 °F]} in the peak waste package temperature, thus prompting the need for a closer look at, and treatment of, the heat transfer characteristics of the natural backfill. This task estimates waste package temperature using a representation of natural backfilling because of drift degradation. The bounding analyses for engineered backfill showed a substantially higher peak waste package temperature than those for natural backfill. This is because with engineered backfill, the space between the drip shield and the rock wall is completely backfilled from the time of repository closure. Whereas, with natural backfill, the space between the drip shield and the rock wall is filled over time.

The natural backfill material is likely to have a large variation in rock/particle sizes, potentially varying from 1 m [3.28 ft] in diameter to a few microns. The particle sizes and shapes determine the regime over which convective heat transfer may be the dominant heat transfer mechanism, and uncertainties in the particle size distribution may result in the heat transfer ranging from pure conduction-dominated heat transfer to convection-dominated heat transfer.

The waste package temperature, computed using selected parameter ranges, suggests sensitivity to the presence or absence of a hypothetical backfill. For the parameter ranges used in this calculation, an estimated peak mean temperature difference of

48 °C [86 °F] was estimated between the peak conduction-only temperature {217 °C [423 °F]} and the peak no backfill temperature {169 °C [336 °F]}.

7. ACKNOWLEDGMENTS

This paper was prepared to document work performed CNWRA for the NRC under Contract No. NRC–02–02–012. The activities reported here were performed on behalf of the NRC Office of Nuclear Material Safety and Safeguards, Division of High-Level Waste Repository Safety. This paper is an independent product of CNWRA and does not necessarily reflect the views or regulatory position of NRC.

8. REFERENCES

1. Gute, G.D., G. Ofoegbu, F. Thomassy, S. Hsiung, G. Adams, A. Ghosh, B. Dasgupta, A.H. Chowdhury, and S. Mohanty. MECHFAIL: A total-system performance assessment code module for evaluating engineered barrier performance under mechanical loading conditions. CNWRA 2003-06. San Antonio, Texas: CNWRA. 2003.

2. NRC. 2004. Risk isights baseline report. ML040560162. Washington, DC: NRC. <www.nrc.gov/waste/hlw-disposal/reg-initiatives/resolve-key-tech-issues.html>

3. DOE. 2000. Abstraction of NFE Drift Thermodynamic Environment and Percolation Flux. ANL–EBS–HS–000003. Rev. 00 ICN 01. Las Vegas, Nevada: DOE.

4. Fedors, R.W., G.R. Adams, C. Manepally, and R.T. Green. 2003. Thermal conductivity, edge cooling, and drift degradation—abstracted model sensitivity analyses for Yucca Mountain. CNWRA Report. San Antonio, Texas: CNWRA.

5. Mohanty, S., G. Adams, and M. Menchaca. 2005. An abstracted model for estimating temperature and relative humidity in the potential repository at Yucca Mountain. Submitted for publication in *Journal of Heat Transfer.*

6. Civilian Radioactive Waste Management System, Management and Operating Contractor. 1999. License application design selection report. B00000000–01717–4600– 00123. Revision 01. Las Vegas, Nevada: Civilian Radioactive Waste Management System, Management and Operating Contractor.

7. Burmeister, L.C. 1993. Convective heat transfer, second edition. New York, New York: John Wiley and Sons.

8. Lapwood, E.R. 1948 Convection of a Fluid in a Porous Medium. *Proc. Camb. Phil. Soc.* 44: 508–521.

9. Panda, M.N. and L.W. Lake. 1994. Estimation of Single Phase Permeability from Parameters of Particle-Size Distribution. AAPG Bulletin. *American Association of Petroleum Geologist.* 78: 1,028–1,039.

10. Krumbein, W.C. and G.D. Monk. 1942. Permeability as a function of the size parameters of unconsolidated sand. *Petroleum Technology.* 5: 1–11.

11. Krumbein, W.C. 1936. Application of logarithmic moments to size frequency distribution of sediments. *Journal of Sedimentary Petrology.* 6: 35–47.

12. Bejan, A. 1984. Convection heat transfer. New York, New York: John Wiley and Sons.

13. Caltagirone, J.P. 1976. Thermo-convective instabilities in a porous medium bounded by two concentric horizontal cylinders. *Journal of Fluid Mechanics.* 78: 337–362.

14. Incropera, F.P. and D.P. DeWitt. 1995. Fundamentals of heat and mass transfer. 3rd Edition. New York, New York: John Wiley and Sons.

15. Manteufel, R.D. 1997. Effects of ventilation and backfill on mined waste disposal facility. *Nuclear Engineering and Design*. 172: 205–219.

16. Press, W.H., S.A. Teukolsky, W.T. Vettering, and B.P. Flannery. 1992. Numerical recipes. Second Edition. Cambridge University Press.

17. Mohanty, S., T.J. McCartin, and D. Esh. Total-system performance assessment (TPA) version 4.0 code: module descriptions and user's guide. San Antonio, Texas: CNWRA. 2002.

18. Lake, L.W. 1989. Enhanced oil recovery. Englewood Cliffs, New Jersey: Prentice Hall.